

## Invisible detergents for structure determination of membrane proteins by small-angle neutron scattering

Søren Roi Midtgaard<sup>1\*</sup>, Tamim A. Darwish<sup>2\*</sup>, Martin Cramer Pedersen<sup>1,3</sup>, Pie Huda<sup>1†</sup>, Andreas Haahr Larsen<sup>1</sup>, Grethe Vestergaard Jensen<sup>1</sup>, Søren Andreas Røssel Kynde<sup>1</sup>, Nicholas Skar-Gislinge<sup>1</sup>, Agnieszka Janina Zygałło Nielsen<sup>4</sup>, Claus Olesen<sup>5</sup>, Mickael Blaise<sup>6,7</sup>, Jerzy Józef Dorosz<sup>8</sup>, Thor Seneca Thorsen<sup>8</sup>, Raminta Venskutonytė<sup>8</sup>, Christian Krintel<sup>8</sup>, Jesper V. Møller<sup>9,13</sup>, Henrich Frielinghaus<sup>10</sup>, Elliot Paul Gilbert<sup>11</sup>, Anne Martel<sup>12</sup>, Jette Sandholm Kastrup<sup>8</sup>, Poul Erik Jensen<sup>4</sup>, Poul Nissen<sup>13,14\*</sup>, Lise Arleth<sup>1\*</sup>

- 1) Structural Biophysics, X-ray and Neutron Science, The Niels Bohr Institute, University of Copenhagen, Denmark
- 2) National Deuteration Facility, Australian Nuclear Science and Technology Organization, Lucas Heights, Australia
- 3) Department of Applied Mathematics, Research School of Physics and Engineering, Australian National University, Canberra ACT 2601, Australia.
- 4) Copenhagen Plant Science Center, University of Copenhagen, Denmark
- 5) Department of Biomedicine, Aarhus University, Denmark
- 6) Institut de Recherche en Infectiologie de Montpellier, Université de Montpellier, France
- 7) Centre for Carbohydrate Recognition and Signaling, Department of Molecular Biology, Aarhus University, Denmark
- 8) Department of Drug Design and Pharmacology, Faculty of Health and Medical Sciences, University of Copenhagen, Denmark
- 9) Department of Biomedicine, Aarhus University, Denmark
- 10) Forschungszentrum Jülich GmbH, TUM FRM-2, Garching, Germany
- 11) Australian Centre for Neutron Scattering, Australian Nuclear Science and Technology Organization, Lucas Heights, Australia
- 12) Institut Laue-Langevin, Grenoble, France
- 13) Department of Molecular Biology and Genetics, Centre for Membrane Pumps in Cells and Disease – PUMPKin, Danish National Research Foundation, Aarhus University, Denmark
- 14) DANDRITE, Nordic-EMBL Partnership for Molecular Medicine, Aarhus University, Denmark

This article has been accepted for publication and undergone full peer review but has not been through the copyediting, typesetting, pagination and proofreading process, which may lead to differences between this version and the Version of Record. Please cite this article as doi: 10.1111/febs.14345

This article is protected by copyright. All rights reserved.

Article type : Original Article

\* To whom correspondence should be addressed:

Dr. S. R. Midtgaard: soromi@nbi.ku.dk

Dr. T. Darwish: tde@ansto.gov.au

Prof. P. Nissen: pn@mbg.au.dk

Prof. L. Arleth: arleth@nbi.ku.dk

†: Current address: Centre for Advanced Imaging, The University of Queensland, Brisbane, Australia

Abbreviations:

SANS: Small-Angle Neutron Scattering

Cryo-EM: Cryo Electron Microscopy

DDM: n-dodecyl- $\beta$ -D-maltopyranoside

OG: octyl  $\beta$ -D-glucopyranoside

bR: Bacteriorhodopsin

LamB: Maltoporin

PSI: Photosystem I

GluA2: Ionotropic glutamate receptor A2

SERCA: Sarco/endoplasmic reticulum  $\text{Ca}^{2+}$  ATPase

MW: Molecular Weight

$R_g$ : Radius of Gyration

$D_{\max}$ : Maximum distance

SEC: Size

kDa: Kilo Dalton

SAXS: Small-Angle X-ray Scattering

FWHM: Full Width Half Maximum

SI: Supplemental Information

Keywords:

Small-Angle Neutron Scattering

SANS

Membrane Proteins

Deuteration

Contrast Matching

## Abstract

A novel and generally applicable method for determining structures of membrane proteins in solution via small-angle neutron scattering (SANS) is presented. Common detergents for solubilizing membrane proteins were synthesized in isotope-substituted versions for utilizing the intrinsic neutron scattering length difference between hydrogen and deuterium. Individual hydrogen/deuterium levels of the detergent head and tail groups were achieved such that the

formed micelles became effectively invisible in heavy water ( $D_2O$ ) when investigated by neutrons. This way, only the signal from the membrane protein remained in the SANS data. We demonstrate that the method is not only generally applicable on five very different membrane proteins but also reveals subtle structural details about the sarco/endoplasmic reticulum  $Ca^{2+}$  ATPase (SERCA). In all, the synthesis of isotope-substituted detergents makes solution structure determination of membrane proteins by SANS and subsequent data analysis available to non-specialists.

## Introduction

Biological membranes form the barrier between internal and external environments of cells and create the separation of compartments and organelles within the cell. They are functionalized by a plethora of membrane proteins that include structural proteins, receptors, channels, active transporters and proteolytic enzymes. Studies of the structure and conformational changes related to the function of membrane proteins therefore represent very important problems in molecular cell biology. Structural studies usually require that the membrane protein of interest is removed from the native membrane, isolated and purified to homogeneity. This requires that the amphipathic membrane protein is stabilized in solution. Multiple systems, including traditional detergents[1], bicelles[2,3], peptide discs[4], amphiphilic polymers[5,6] and nanodiscs[7] are available for this purpose. While detergents and bicelles have been useful for Cryo-EM[8], NMR[9] and crystallization experiments[1], the comparatively monodisperse nanodisc particles are promising in combination with small-angle scattering and allows low-resolution structural information of the membrane protein to be obtained under solution conditions[10–12]. However, reconstitution of membrane proteins in nanodiscs remains a challenge with respect to obtaining sufficiently homogeneous samples for scattering experiments. In our attempt to find a more general and easily applicable solution to these problems, the use of detergents was re-examined and combined with our previously developed idea of a “stealth”-carrier for SANS studies of membrane proteins[10]. The detergents, octyl  $\beta$ -D-glucopyranoside (OG) and n-dodecyl- $\beta$ -D-maltopyranoside (DDM) that are both compatible with membrane protein reconstitution were deuterated through a new synthesis method that allowed for selective deuteration of the two detergents to different predetermined levels at the hydrophilic headgroups and hydrophobic tails. To obtain the best possible SANS signal-to-noise of the membrane protein structure, the different parts of the detergents were deuterated such that they had the same neutron scattering length density as 100% deuterium oxide ( $D_2O$ ). This way the obtained SANS data of membrane proteins stabilized in these detergents in  $D_2O$  only consists of the single contrast signal stemming from the purified membrane protein.

The general idea to use the contrast match-point of a detergent or surfactant to study membrane protein structures has previously been investigated[13–29]. However, a common feature for all previous studies is that they rely on commercially available hydrogenated detergents or fully deuterated detergents developed for different purposes. This is reflected in the resulting neutron scattering data, which include scattering cross-terms from the entire detergent-membrane protein complex due to the differences in excess scattering length density of the hydrophobic and hydrophilic parts of the detergents present on length scales of 10-20 Å. This effect is difficult to disentangle from the signal from the membrane protein and significantly limits the resolution that can be obtained. In addition, the overall match-point of the commercially available detergents is generally different from that of 100%  $D_2O$ , hence yielding additional incoherent scattering

background from the hydrogen in the buffer. While the studies have provided overall shape parameters of studied membrane proteins[14,20,21,24,27,28], their finer structure could not be extracted from the data due to these factors.

In this study, two commonly used detergents, OG and DDM, were synthesized with varying deuteration levels in head- and tailgroups such that they were fully match-out deuterated in D<sub>2</sub>O buffer when investigated by SANS. This yielded SANS data where only the membrane proteins were visible. The practical workflow is outlined in figure 1.

Initially, the membrane protein is purified in hydrogenated buffer and hydrogenated detergent. This step ensures that as many impurities as possible are removed before the more expensive deuterated buffers are introduced. Afterwards, a size exclusion purification in the equivalent deuterated buffer and match-out deuterated detergent is performed. This step ensures that the hydrogenated detergent and buffer are fully exchanged to the deuterated counterparts (see SI 3 for details). Furthermore, any aggregated protein that might be present in the sample arising from e.g. freezing, transport, etc., is also removed to ensure optimal data quality. The peak fraction from the buffer and detergent exchange is collected and, without further manipulation, measured by SANS. Scattering data obtained this way can be reduced and subsequently analyzed by a number of available programs for small-angle scattering (such as ATSAS[30], WillItFit[31], SASSIE[32], IRENA[33], FoXS[34] etc.) due to the simplified contrast situation achieved through the use of *de facto* invisible detergents.

## Results

### Detergent deuteration.

As described above, the chosen deuterated detergents were two commonly used sugar based detergents, namely OG and DDM. The partial specific molecular volumes of hydrophilic head and hydrophobic tail groups were determined by densitometry (see SI 1 for details) such that the deuteration level for complete match-out at 100% D<sub>2</sub>O at 20 °C could be calculated (see table 1). Custom syntheses were then developed to produce the desired partially deuterated versions of both detergents.

### Synthesis of detergents with controlled deuteration levels in hydrophilic headgroups and hydrophobic tails

Each of OG and DDM is made of two parts; the C8 or C12 alkyl chain tail and the corresponding sugar heads of glucose and maltose, respectively. In the case of OG, the required deuteration levels in the octyl chain and the glucose sugar head (7 non-exchangeable positions) groups were 94% D and 52% D, respectively. In DDM, the required deuteration levels in the dodecyl chain and the maltose sugar head (14 non-exchangeable positions) groups were 89% D and 57% D, respectively. Deuterating the detergent molecules directly using hydrothermal reactions was not possible as the harsh conditions of high temperature and pressure were incompatible with the delicate nature of the molecules. The deuteration of methylene units in alkyl hydrocarbons can only be achieved using forced conditions of a hydrothermal catalytic exchange reaction[35], while the deuteration of the sugar groups can be achieved using milder reaction conditions[36]. An alternative approach of deuterating the

corresponding sugar molecule and the alkyl chains separately before attaching them together would not be feasible since the sugar groups, glucose and maltose, are reducing sugars, which means they would quickly decompose in the presence of reducing reagents due to the hydrolysis of their hemiacetal moieties. Reducing sugars must be preceded by conversion into glycoside to prevent reduction at the anomeric carbon when exposed to Raney Nickel[36]. Therefore, to achieve specific deuteration levels in the two different parts of any of the two detergent molecules, it was necessary to follow a multiple-step synthesis approach and two sequential deuteration steps. This involved (illustrated in figure 2 for OG): **A**) deuterating the alkyl chain at the required deuteration level starting from the corresponding fatty acid and using hydrothermal Pt/C catalyzed H/D exchange reactions at 220°C in the appropriate molar ratio of deuterium and hydrogen atoms in the mixture; **B**) reducing the fatty acid molecule to the corresponding alcohol and attaching the deuterated alcohol to the corresponding acetylated bromo-sugar head group (i.e., 2,3,4,6-tetra-O-acetyl- $\alpha$ -D-glucopyranosyl bromide and 2,3,6,2',3',4',6'-hepta-O-acetyl- $\alpha$ -D-maltosyl bromide) according to standard procedures; **C**) deacetylation of the sugar head group followed by deuterating it to achieve the required deuteration level by using mild conditions of Raney Nickel as a catalyst in D<sub>2</sub>O/H<sub>2</sub>O mixture at 80°C for 18 h. The latter step allows the incorporation of deuterium atoms on carbons adjacent to free hydroxyl groups ( $\alpha$  positions) in the sugar head group with retention of configuration, but it does not affect any H/D back-exchange at the more inert alkyl chain sites[36–38] (see SI 2 for details).

#### **SANS contrast variation on empty micelles**

The deuteration levels obtained from the custom synthesis were close to the desired values (Table 1), implying that the scattering length density from the detergents should theoretically be close to that of 100% D<sub>2</sub>O. To experimentally verify this, micelles of the match-out deuterated detergents were measured by SANS in a set of buffers with D<sub>2</sub>O content ranging from 60% to 100%. Experiments were performed at ANSTO and FRMII (See SI 4). Background subtracted data are plotted in figure 3.

The SANS intensity from both detergents is reduced by more than two orders of magnitude when changing the percentage of D<sub>2</sub>O in the buffer from 60% to 100%. Indeed, at 100% D<sub>2</sub>O, the signal from the match-out deuterated detergents is effectively at the noise-level over the measured  $q$ -range and exhibiting no significant  $q$ -dependence.  $I(0)$  values (figure 3C) were determined by indirect Fourier transformation[39]. The expected parabolic behavior of the  $I(0)$  as a function of D<sub>2</sub>O contents was confirmed (figure 3C) and the match-points were found to be at 102% D<sub>2</sub>O for DDM and 103% D<sub>2</sub>O for OG.

In figures 3D and E the obtained contrast-matched data are compared to previously obtained and published SANS data from the commercially available tail-deuterated counterparts to OG and DDM: d17-OG and d25-DDM[28]. These data, (obtained and plotted with permission from the authors), are measured at the D22 instrument at ILL, France and plotted at their respective match-points which is 90% D<sub>2</sub>O for d17-OG and 85% for d-25-DDM [28].

The data from the tail-deuterated detergent d17-OG exhibit the expected  $q$ -dependence with an oscillation having a maximum at around  $0.15 \text{ \AA}^{-1}$ , but overall a very low intensity of the  $I(q)$  at the match-point. Note however, that the d17-OG data had a small experimental discrepancy between the background levels of the measured buffer and sample. Due to the low signal to background ratio, this had relatively large impact on the obtained scattering intensity as illustrated in fig 3D

which plots both the d17-OG data with background subtracted using the theoretical normalization (light grey curve) and the same data with a small renormalization of the background (dark grey curve). As it is seen, this causes a relatively large shift in the overall scattering intensity, which unfortunately makes a direct quantitative comparison to our data difficult (figure 3D). In any case, the density fluctuations expected in the d17-OG are systematic and clearly visible in the  $I(q)$ -data regardless of the buffer level, while there is no indication of this feature in the data from the match-out deuterated OG.

In the comparison between the d25-DDM at 85% D<sub>2</sub>O and the match-out d-DDM at 100% D<sub>2</sub>O (figure 3E) the above mentioned experimental discrepancy between the buffer and sample background levels is not present to the same extent. Furthermore, a much stronger difference between the custom-synthesized and commercial variants is observed which clearly demonstrates the added value of the custom synthesis of these match-out detergents. Indeed, the scattering intensity of the d25-DDM is 5-6 times as strong around 0.1 Å<sup>-1</sup> as compared to match-out d-DDM and its  $q$ -dependence is, as expected, very significant due to the internal core-shell contrast.

Figure 3F shows the simulated scattering intensity of bR reconstituted in, respectively, a match-out deuterated d-DDM micelle in 100% D<sub>2</sub>O and a d25-DDM micelle at 85% D<sub>2</sub>O. Note that for d25-DDM the overall scattering intensity is lower than for d-DDM. This is a trivial consequence of the different D<sub>2</sub>O concentrations. More importantly, the  $q$ -dependence differs significantly in the two systems. The oscillation around 0.1 Å<sup>-1</sup> arising from the core-shell contrast of the d25-DDM is still visible in the bR-micelle complex, but already from  $q > 0.02$  Å<sup>-1</sup> the two  $I(q)$ -functions start differing (see dashed line in figure 3F) as a result of the internal contrast of the d25-DDM micelles. This is already visible in the Guinier range and show that not even a reliable value for the  $R_g$  of bR can be obtained with the d25-DDM as reconstitution system. Similar effects, though less pronounced are to be expected if using d17-OG as the reconstitution system.

### **Exchange of protonated to deuterated detergents**

The extent of exchange from hydrogenated to deuterated detergents in samples of membrane proteins outlined in figure 1, was evaluated by monitoring the background SANS signal at high  $q$  as a function of SEC flowrate, as the hydrogen from any non-exchanged buffer or detergent would generate an increase in incoherent background scattering. In initial experiments, the background scattering was found to be very high due to incomplete exchange of the detergent. The Agilent Bio SEC-3-300 column, used in combination with a high flowrate (0.7 ml/min) was found to be the cause and a lowering of the flowrate solved to 0.4 ml/min solved the problem. Hence, for this method to perform as intended, it is of paramount importance to use a sufficiently low flowrate in the SEC to enable an enhanced H/D exchange of detergent and solvent (see further details in SI 3).

### **Membrane protein data and analysis.**

To evaluate this method, five structurally different membrane proteins were investigated; bacteriorhodopsin (bR), maltoporin (LamB), photosystem I (PSI), the ionotropic glutamate receptor A2 (GluA2) and the sarco/endoplasmic reticulum Ca<sup>2+</sup> ATPase (SERCA). The first three proteins, bR, LamB and PSI are all examples of membrane proteins that have either no or small domains outside the cell membrane. These three proteins were also chosen as they are relatively stable and at the same time representative of the wide range of molecular weights found in membrane proteins viz. ~27 kDa (bR), ~47 kDa (LamB) and ~650 kDa (PSI). Two additional membrane proteins, GluA2 (~385

kDa) and SERCA (~110 kDa), were selected as examples of more unstable membrane proteins with complex structures and large protein domains outside the membrane spanning region that may be captured in distinct functional states. SANS data on the LamB protein was obtained on the QUOKKA instrument at ANSTO, GluA2 was measured on KWS1 at FRM-II and data from bR, PSI and SERCA were obtained on the D22 instrument at ILL. The SANS data and results obtained using the invisible detergents in 100% D<sub>2</sub>O are presented in figure 4 (See SI 4 for further details).

Crystal structures were available for all proteins, and these were used as a basis for modeling the theoretical scattering patterns to be compared to the experimental data (figure 4). bR was found agree with a dimer structure, LamB with a combination of homo-trimers and higher oligomers of these, PSI data with a monomer structure, GluA2 with a homo-tetramer and SERCA with a combination of two structural states combined with a minor aggregated fraction of SERCA using a previously developed approach[40] (see SI 4 for more details). Hydration layers were added to all water-exposed surfaces. Instrumental resolution effects on the SANS data were taken into account in the analysis[41] and the required values for the  $\Delta q(q)$  for the resolution function calculations for the different instrumental settings were provided by the beamlines. The resolution effect is most clearly visible for the SERCA data where an (expected) discontinuity of the fitted model is observed around  $q=0.03$  1/Å. A constant background and a scale factor were fitted to obtain the best agreement between the data and model, shown in figure 4. The figure also plots the theoretical pair distance distribution functions  $p(r)$  calculated from the fitted models together with the ones obtained from the data by indirect Fourier transformation[39]. The values of radius of gyration,  $R_g$ , and maximum internal distances,  $D_{max}$ , obtained from the  $p(r)$  functions, are listed in table 2 together with molecular masses estimated from the estimated porod volume and the partial specific molecular volume found by Mylonas *et al.*[42]. Table 2 compares these values to the theoretical  $R_g$ ,  $D_{max}$  and  $MW$ -values based on the available crystal-structures. Note that the experimental estimates for the Porod volume are not expected to have a precision better than  $\pm 20\%$ [30]. Finally, *Ab initio* bead modelling was performed for bR, PSI and GluA2 and compared with the known structures (See Fig 4 and SI 4).

bR with a monomeric molecular weight of ~27 kDa, is a relatively small membrane protein with seven transmembrane helices. Due to its small size, it scatters weakly and any interfering signal from the detergent should be visible in the data. As is evident from figure 4, the experimental data correspond well with a dimer of bR (PDB ID: 1PY6). While bR is traditionally found as a monomer or trimer, a dimeric form is well documented[43]. A closer look into the structural parameters in table 2, show that the experimentally obtained  $R_g$ ,  $D_{max}$  and  $MW$ -values are generally slightly larger than what would be expected from the crystal structures of the dimer. This larger size is also indicated in the obtained *ab initio* structure (figure 4) and can both be indications of slightly more loose or open dimer-structures in solution than in the crystals, but may also indicate the presence of small populations of higher order oligomers. These questions could be pursued further in a future work. However, the ability to discern the oligomeric state show that the method can probe the structure of relatively small membrane proteins in solution without any significant contribution from the match-out deuterated detergent. bR has the same size and general fold as many G-protein coupled receptors (GPCRs)[44]. The data shows that this interesting class of membrane proteins, typically too small for cryo-EM fall well within the range of this SANS-based method.

The LamB protein is a simple beta barrel porin structure with a monomer weight of  $\sim 47$  kDa[45], hence a membrane protein with intermediate molecular weight. The SANS data presented in figure 4 were found to agree with an oligomeric mixture of monomer, trimer and heptameric states of the underlying LamB homo-trimer (PDB ID: 1MAL, See SI 4 for further details), making an *ab initio* structure irrelevant. While it is clear from the data and the values for  $R_g$ ,  $D_{max}$  and  $MW$  listed in table 2 that the data must arise from, on average, larger particles than the basic LamB homo-trimeric structure, another base set of structures derived from the homo-trimer could likely also have provided a good representation of the measured data. A small deviation between the model and data is visible at  $0.11 \text{ \AA}^{-1}$ , this hints towards the possibility of investigating finer structural details of the LamB oligomerization with this method. However, a larger set of data would be required for this purpose.

Plant PSI is a large protein complex with a diameter of around 20 nm that comprises multiple, mostly alpha-helical subunits[46,47]. It is evident from the SANS data in figure 4 that the overall structure of PSI in solution is highly similar to the one recently found by X-ray crystallography (PDB ID: 4RKU). Interestingly, a small discrepancy is found around  $0.1 \text{ \AA}^{-1}$  and the experimental values for  $R_g$  and  $D_{max}$  are slightly higher than the comparable value for the crystal structure. The slightly larger size observed by SANS is also reflected in the plotted *ab initio* structure (fig 4). The observed differences likely stem from the fact that  $\sim 10\%$  of the amino acid residues are not found in the crystal structure. Other contributing factors could be that the solution structure, due to increased flexibility, is slightly different from the one confined in the crystal or that the crystal structure is from pea PSI and the SANS data was obtained from barley PSI. In either case, it is interesting that this method is able to demonstrate minor discrepancies between the known model and the obtained SANS data for this otherwise highly studied membrane protein complex.

GluA2 is a neurotransmitter activated receptor with a structure consisting of a large, extended homo-tetramer[48]. The scattering data correspond very well with the known structure of GluA2 (PDB ID: 4U2P), which is also seen from the resemblance between the crystal structure and the *ab initio* model (see figure 4) and from the good agreement (within the experimental accuracy) between the experimental and expected values for the  $R_g$ ,  $D_{max}$  and  $MW$  listed in table 2. The values found in table 2 also indicate a good agreement with the expected structure within the expected accuracy. This demonstrates that the method can readily probe the structure of large and complicated membrane proteins and, in this case, confirm that the crystal structure is representative of the solution structure.

SERCA is a calcium transporting ATPase and more difficult to stabilize in solution than the other proteins in this study. It has a complex fold with three major cytoplasmic domains outside the membrane spanning region that rearrange with respect to each other during the calcium transport cycle[49]. Several of the structural states relating to the pumping cycle of SERCA have been revealed by crystallography via stabilization with co-factors and inhibitors[50]. However, some states and dynamic transitions are still debated. Here the structure in the absence of calcium and stabilized by the non-hydrolysable ATP analog AMPPCP has been investigated, representing the so-called E1 and E2 states. High quality SANS data has been collected as evidenced by the relatively small error bars and the presence of significant features in the high- $q$  region. The data correspond to monomeric SERCA together with a minor fraction of oligomeric SERCA ( $\sim 2\%$  of the molecules, see SI 4 for details). The data clearly delineate calcium-free SERCA structures, as is also evident from the

enhanced view in figure 4 where the structure with calcium (PDB ID: 1T5S) completely fails to describe the finer details observed in the experimental data. The structural state probed in this study is expected to be dynamic and potentially switch between the E2 (PDB ID: 4UU1) and E1 (PDB ID: 4H1W) calcium-free states[50]. Fitting the individual E2 and E1 states and a superposition of the two structures to the data indeed reveals that while both the calcium-free states represent the features in the data better than the calcium-bound form, the best description of the data is obtained by a linear combination of the E2 and E1 states with a distribution of 50% E2 and 50% E1 (see SI 4 for details). Not only does this confirm what has been previously suggested in the literature but also provides a result that could not have been obtained using a traditional crystallographic approach. Additionally, this result demonstrates that the workflow and method presented here is compatible with probing the finer structure of this challenging and unstable type of membrane proteins. There was aggregation in the SERCA sample, as clearly seen from the experimental data in figure 4, and reflected in the  $R_g$ ,  $D_{max}$  and  $MW$  listed in table 2. This effect was included in the modelling as a structure factor and using a previously developed approach[40]. However, since the two structures of interest, E1 and E2, had approximately the same size, and hence the same scattering intensity at low- $q$ , the aggregation did not affect the assessment of the equilibrium between these states. A detailed description of the data analysis, the structure factor as well as a more thorough discussion of this matter can be found in the supplemental information (SI 4).

## Discussion

The feasibility of using custom synthesized match-out deuterated detergents for elucidating the structure of membrane proteins by solution SANS has been demonstrated. Firstly, the synthesis of partly deuterated versions of DDM and OG were developed and the desired match-out deuteration confirmed by SANS. Secondly, the detergents were successfully used for stabilizing membrane proteins while performing SANS experiments. Thirdly, by analysis of the obtained SANS data, it was demonstrated that this method does indeed perform as well as expected and hence provides a novel and easy-to-use tool for low-resolution structural studies of membrane proteins. For the past decade, performing a SAXS experiment to complement high-resolution structural work by crystallography has become a standard approach when investigating soluble proteins[51]. This is not least due to the easy analysis made possible by the ATSAS suite[30] and development of stable and high throughput SAXS beamlines[52]. This approach is now directly transferable to membrane proteins by using the approach of deuterated detergents and SANS.

The method of using match-out deuterated detergents to obtain solution structures of membrane proteins fills an important gap in the toolbox for their detailed investigation. While traditional protein crystallography has undeniably produced fantastic new insights into biological processes over several decades, obtaining crystals of membrane proteins diffracting to high resolution remains a bottleneck[53]. Indeed, larger flexible membrane proteins are under-represented in the protein data bank due to this obstacle. The method presented here allows for probing the structure in detail early in the process when a robust expression and purification protocol has been established. Recent advances in both the methodology and hardware have matured Cryo-EM to a technique that has become a major game changer in structural biology[8]. However, a major drawback of Cryo-EM is the requirement of proteins with a molecular mass above  $\sim 100$ -150 kDa to obtain sufficiently high signal-to-noise ratios to allow for the alignment and averaging of the individual frames required for obtaining the desired high resolution data[8]. This means that many important membrane proteins

are too small for Cryo-EM. NMR is also a popular method for determining the high resolution structure of membrane proteins[54], but due to the overcrowding of the spectra, only relatively small proteins (~20-30 kDa) may be solved. Hence, the combined SANS and invisible detergent method described in this paper provides an easily applicable alternative that allows for analyzing protein structures with a resolution down to about 10 Å, and that importantly contributes to bridging the gap between existing methods.

Several other strategies have been proposed in the literature which utilize some of the aspects of the method presented here. The use of small-angle X-ray scattering (SAXS) for elucidating the structure of membrane proteins in detergent micelles has been thoroughly tested[55–58] but thus far mainly revealed information on the detergent rim around the membrane proteins. Furthermore, using so-called nanodiscs coupled with small-angle scattering has also been shown to be possible but the sample preparation remains challenging[11,59]. This is contrasted with the approach presented here, where the sample preparation is uncomplicated and the signal almost exclusively comes from the membrane protein, significantly simplifying the data analysis and increasing the information that can be extracted about the structure of the investigated membrane protein. Importantly, this method allows for probing the structure of un-crystalizable dynamic structural states of proteins. Recent technical developments in SEC-SANS sample environments will furthermore allow for performing the whole workflow outlined in figure 1 *in situ* at the neutron instrument, together with removing any oligomeric species caused by unstable proteins[60].

Five different membrane proteins and two detergents were investigated in this study. The data demonstrate the general applicability of the approach and provide promising perspectives for future use. The basic idea of match-out deuteration may easily be generalized to other detergent types to accommodate special needs for particular membrane proteins or in combination with selective deuteration of different subunits.

### **Acknowledgements**

The authors acknowledge Dr. Robert Knott at ANSTO and Dr. Adam Round at ESRF for their assistance in obtaining supporting SAXS data. We thank ANSTO, ILL and FRM II for awarding us beamtime for this project at, respectively, the QUOKKA, D22 and KWS-1 instruments. R.V., C.K., T.S.T., J.J.D and J.S.K. thank Eric Gouaux for providing the GluA2cryst construct and protein purification protocol. Dr. Frank Gabel and Dr. Christine Ebel is thanked for kindly providing data on the tail-deuterated detergents previously published in [28]. PhD student Nicolai Tidemand Johansen is thanked for helping with the SANS measurements of GluA2. We thank the Danish Agency for Science, Technology and Innovation funding agency for making this study possible through a Sapere Aude grant to L.A.. R.V., C.K., and J.S.K. acknowledge the support from the Lundbeck Foundation, The Danish Council for Independent Research – Medical Sciences and GluTarget. The authors also acknowledge financial support from the Center for Synthetic Biology (bioSYNergy) funded by the UCPH Excellence Programme for Interdisciplinary Research and to the Lundbeck foundation “BRAINSTRUC” center.

## Author Contributions

S.R.M., T.D. and L.A. conceived the project. T.D. developed methods and synthesized the deuterated detergents. S.R.M., A.J.Z.N., P.E.J., M.B., C.O., P.N., R.V., T.S.T., J.J.D., C.K., J.S.K. produced and provided proteins. S.R.M., M.C.P., S.A.R.K., P.H. A.H.L. performed the experiments. A.H.L., N.S.G., G.V.J., M.C.P., S.A.R.K performed the data analysis. H.F., E.G. and A.M. were SANS instrument responsible and participated in the SANS measurements. S.R.M., T.D. and L.A. co-wrote the paper.

## Competing Financial Interests

The authors declare no competing financial interests.

## Methods

### General Materials

Hydrogenated Octyl- $\beta$ -D-glucopyranoside (OG) was purchased from Applichem while hydrogenated n-dodecyl- $\beta$ -D-maltopyranoside (DDM) was purchased from Sigma Aldrich. Match-out deuterated detergents were custom synthesized as described briefly below and in detail in the supplemental information. The membrane proteins used in the present study were expressed and purified according to standard protocols as described the supplemental information. All pH values have been measured using a standard glass electrode and all reported values are from the direct measurement[61].

### Densitometry

Densitometry was performed using a DMA 5000 density meter (Anton Paar). Octyl- $\beta$ -D-glucopyranoside (OG) (Sigma-Aldrich) was solubilized in 20 mM Tris/HCl, pH 7.5 and 100 mM NaCl in concentrations of 25 and 100 mM. n-dodecyl- $\beta$ -D-maltopyranoside (DDM) (Sigma-Aldrich) was solubilized in identical buffer at concentrations of 15 and 60 mM. All samples were prepared in triplicates and measured at 4°C intervals between 4°C and 28°C. See further details in the supplemental information.

### General detergent synthesis

Chemicals and reagents of the highest grade were purchased from Sigma-Aldrich and Carbosynth Limited (Berkshire, UK) and were used without further purification. Solvents were purchased from Sigma-Aldrich and Merck and were purified by established methods[62]. NMR solvents were purchased from Cambridge Isotope Laboratories Inc. and Sigma-Aldrich and were used without further purification. D<sub>2</sub>O (99.8 %) was supplied by Sigma-Aldrich. Thin-layer chromatography (TLC) was performed on Fluka Analytical silica gel aluminium sheets (25 F254). Davisil® silica gel (LC60Å 40-63 micron) was used for bench-top column chromatography.

Deuteration of octanoic acid and dodecanoic acid was performed using hydrothermal H/D exchange reactions in D<sub>2</sub>O at 220°C by mixing the appropriate amount of fatty acid with NaOD and Pt/C (10 % w/w) in a Mini Benchtop 4560 Parr Reactor (600 mL vessel capacity, 3000 psi maximum pressure, 350 °C maximum temperature). This was followed by filtering the catalyst, acidifying the solution

and then extracting the aqueous phase with ethyl acetate. Thin layer chromatography was used (referenced with the protonated compound) to estimate the purity and to develop separation protocols.  $^1\text{H}$  NMR (400 MHz),  $^{13}\text{C}$  NMR (100.6 MHz) and  $^2\text{H}$  NMR (61.4 MHz) spectra were recorded on a Bruker 400 MHz spectrometer at 298 K. Chemical shifts, in ppm, were referenced to the residual signal of the corresponding NMR solvent. Deuterium NMR was performed using the probe's lock channel for direct observation. Electrospray ionization mass spectra (ESI-MS) were recorded on a 4000 QTrap AB Sciex spectrometer. The overall percentage deuteration of the molecules was calculated by MS using the isotope distribution analysis of the different isotopologues. This was calculated taking into consideration the  $^{13}\text{C}$  natural abundance, whose contribution was subtracted from the peak area of each M+1 isotopologue to allow for accurate estimation of the percentage deuteration of each isotopologue.

### **Transfer of membrane proteins into deuterated detergents**

The transfer was performed using an Agilent Bio SEC-3-300 column with a flowrate of 0.4 ml/min. The flow through from the column was collected, measured and used for background subtraction.

Buffers used for PSI, GluA2 and bR contained 0.5 mM match-out deuterated DDM, 20 mM Tris/DCl pH 7.5 and 100 mM NaCl in  $\text{D}_2\text{O}$ . For LamB, 40 mM match-out deuterated OG was used instead of DDM. For SERCA, the buffer used consisted of 20 mM MOPS pH 6.8, 100 mM KCl and 0.5 mM DDM.

### **SANS measurements**

SANS measurements of the deuterated OG were performed at KWS 1, Forschungs Neutronenquelle Heinz Maier-Leibnitz, Munich (FRM II). A neutron wavelength of 4.5 Å ( $\pm 10\%$  FWHM) was used at two sample-to-detector distances covering  $q$ -ranges of 0.012–0.16 Å $^{-1}$  and 0.0057–0.077 Å $^{-1}$ . Pre-calibrated plexiglass was used as a standard for absolute calibration of the scattered intensity  $I(q)$  in units of 1/cm, where  $q = (4\pi/\lambda)\sin(\theta)$  and  $2\theta$  is the scattering angle and  $\lambda$  is the wavelength. GluA2 was measured at the same instrument using three sample-to-detector distances: 1.5 m and 4.0 m with 4 m collimation and 8.0 m with 8 m collimation were used.

SANS measurements of the LamB protein in deuterated OG and empty deuterated DDM micelles were performed at QUOKKA[63], Australian Nuclear Science and Technology Organization (ANSTO), Sydney. A neutron wavelength of 5.0 Å ( $\pm 10\%$  FWHM) was used at two sample-to-detector distances, covering  $q$ -ranges of 0.017–0.51 Å $^{-1}$  and 0.0076–0.098 Å $^{-1}$ . Data were absolutely calibrated by an attenuated direct beam transmission measurement of the scattered intensity.

SANS measurements of the bR, SERCA and PSI in deuterated DDM were performed at D22, Institut Laue-Langevin (ILL), Grenoble. A neutron wavelength of 6.0 Å ( $\pm 10\%$  FWHM) was used at two sample-to-detector distances covering  $q$ -ranges of 0.022–0.48 Å $^{-1}$  and 0.0087–0.12 Å $^{-1}$ .  $\text{H}_2\text{O}$  was used as a standard for absolute calibration of the scattered intensity.

## SANS data analysis

Pair distance distribution functions,  $p(r)$  and the associated values for the radius of gyration,  $R_g$ , and maximum particle diameter,  $D_{max}$ , were obtained from the scattering data using a Bayesian indirect Fourier transform[39]. Porod volume based values for the protein molar mass was estimated by the GNOM program of the ATSAS package [64]. *Ab initio* models of the proteins were obtained using the DAMMIF program of the ATSAS package[64]. Theoretical scattering patterns for the relevant protein structures were calculated using the program WillItFit[31]. Hydrogen and deuterium was added to the structures by the Phenix program ReadySet![65], exchanging all labile hydrogens for deuterium. A surface hydration layer was added to the hydrophilic areas of the structures using an in-house routine which identifies surface residues and places beads at a distance of 5 Å from the C $_{\alpha}$  of the surface residues. This routine allows for not adding a water layer at the hydrophobic portion of the protein surface as identified by the Orientations of proteins in Membranes' database (OPM)[66].

- 1 Loll PJ (2014) Membrane proteins, detergents and crystals: what is the state of the art? *Acta Crystallogr. Sect. F Struct. Biol. Commun.* **70**, 1576–1583.
- 2 Diller A, Loudet C, Aussenac F, Raffard G, Fournier S, Laguerre M, Grélard A, Opella SJ, Marassi FM & Dufourc EJ (2009) Bicelles: A natural “molecular goniometer” for structural, dynamical and topological studies of molecules in membranes. *Biochimie* **91**, 744–51.
- 3 Poulos S, Morgan JLW, Zimmer J & Faham S (2015) *Bicelles Coming of Age*, 1st ed. Elsevier Inc.
- 4 Midtgaard SR, Pedersen MC, Kirkensgaard JJK, Sørensen KK, Mortensen K, Jensen KJ & Arleth L (2014) Self-assembling peptides form nanodiscs that stabilize membrane proteins. *Soft Matter* **10**, 738–52.
- 5 Knowles TJ, Finka R, Smith C, Lin Y-P, Dafforn T & Overduin M (2009) Membrane proteins solubilized intact in lipid containing nanoparticles bounded by styrene maleic acid copolymer. *J. Am. Chem. Soc.* **131**, 7484–5.
- 6 Popot J-L, Althoff T, Bagnard D, Banères J-L, Bazzacco P, Billon-Denis E, Catoire LJ, Champeil P, Charvolin D, Cocco MJ, Crémel G, Dahmane T, de la Maza LM, Ebel C, Gabel F, Giusti F, Gohon Y, Goormaghtigh E, Guittet E, Kleinschmidt JH, Kühlbrandt W, Le Bon C, Martinez KL, Picard M, Pucci B, Sachs JN, Tribet C, van Heijenoort C, Wien F, Zito F & Zoonens M (2011) Amphipols from A to Z. *Annu. Rev. Biophys.* **40**, 379–408.
- 7 Ritchie TK, Grinkova Y V, Bayburt TH, Denisov IG, Zolnerciks JK, Atkins WM & Sligar SG (2009) Chapter 11 Reconstitution of Membrane Proteins in Phospholipid Bilayer Nanodiscs. *Methods Enzymol.* **464**, 211–231.
- 8 Nogales E & Scheres SHW (2015) Cryo-EM: A Unique Tool for the Visualization of Macromolecular Complexity. *Mol. Cell* **58**, 677–689.
- 9 Murray DT, Das N & Cross TA (2013) Solid state NMR strategy for characterizing native membrane protein structures. *Acc. Chem. Res.* **46**, 2172–2181.
- 10 Maric S, Skar-Gislinge N, Midtgaard S, Thygesen MB, Schiller J, Frielinghaus H, Moulin M, Haertlein M, Forsyth VT, Pomorski TG & Arleth L (2014) Stealth carriers for low-resolution structure determination of membrane proteins in solution. *Acta Crystallogr. D. Biol. Crystallogr.*

70, 317–28.

- 11 Kynde SAR, Skar-Gislinge N, Pedersen MC, Midtgaard SR, Simonsen JB, Schweins R, Mortensen K & Arleth L (2014) Small-angle scattering gives direct structural information about a membrane protein inside a lipid environment. *Acta Crystallogr. D. Biol. Crystallogr.* **70**, 371–83.
- 12 Skar-Gislinge N, Kynde SAR, Denisov IG, Ye X, Lenov I, Sligar SG & Arleth L (2015) Small-angle scattering determination of the shape and localization of human cytochrome P450 embedded in a phospholipid nanodisc environment. *Acta Crystallogr. Sect. D Biol. Crystallogr.* **71**, 2412–2421.
- 13 Nawroth T, Dose K & Conrad H (1989) Neutron small angle scattering of detergent solubilized and membrane bound ATP-synthase. *Phys. B Condens. Matter* **156–157**, 489–492.
- 14 Sverzhinsky A, Qian S, Yang L, Allaire M, Moraes I, Ma D, Chung JW, Zoonens M, Popot JL & Coulton JW (2014) Amphipol-Trapped ExbB-ExbD Membrane Protein Complex from *Escherichia coli*: A Biochemical and Structural Case Study. *J. Membr. Biol.*, 1005–1018.
- 15 Wise DS, Karlin a & Schoenborn BP (1979) An analysis by low-angle neutron scattering of the structure of the acetylcholine receptor from *Torpedo californica* in detergent solution. *Biophys. J.* **28**, 473–496.
- 16 Le RK, Harris BJ, Iwuchukwu IJ, Bruce BD, Cheng X, Qian S, Heller WT, O’Neill H & Frymier PD (2014) Analysis of the solution structure of *Thermosynechococcus elongatus* photosystem i in n-dodecyl- $\beta$ -d-maltoside using small-angle neutron scattering and molecular dynamics simulation. *Arch. Biochem. Biophys.* **550–551**, 50–57.
- 17 Hunt JF, McCrea PD, Zaccai G & Engelman DM (1997) Assessment of the aggregation state of integral membrane proteins in reconstituted phospholipid vesicles using small angle neutron scattering. *J. Mol. Biol.* **273**, 1004–1019.
- 18 Wang ZY, Muraoka Y, Nagao M, Shibayama M, Kobayashi M & Nozawa T (2003) Determination of the B820 subunit size of a bacterial core light-harvesting complex by small-angle neutron scattering. *Biochemistry* **42**, 11555–11560.
- 19 Gall A, Dellerue S, Lapouge K, Robert B & Le L (2001) Scattering Measurements on the Membrane Protein Subunit B777 in a Detergent. *Biopolymers* **58**, 231–234.
- 20 Cardoso MB, Smolensky D, Heller WT & O’Neill H (2009) Insight into the structure of light-harvesting complex II and its stabilization in detergent solution. *J. Phys. Chem. B* **113**, 16377–16383.
- 21 Clifton L a., Johnson CL, Solovyova AS, Callow P, Weiss KL, Ridley H, Le Brun AP, Kinane CJ, Webster JRP, Holt S a. & Lakey JH (2012) Low resolution structure and dynamics of a colicin-receptor complex determined by neutron scattering. *J. Biol. Chem.* **287**, 337–346.
- 22 Pachence JM, Edelman IS & Schoenborn BP (1987) Low-angle neutron scattering analysis of Na/K-ATPase in detergent solution. *J. Biol. Chem.* **262**, 702–709.
- 23 Perkins SJ & Weiss H (1983) Low-resolution structural studies of mitochondrial ubiquinol:cytochrome c reductase in detergent solutions by neutron scattering. *J. Mol. Biol.* **168**, 847–866.
- 24 Gabel F, Lensink MF, Clantin B, Jacob-Dubuisson F, Villeret V & Ebel C (2014) Probing the conformation of FhaC with small-angle neutron scattering and molecular modeling. *Biophys. J.*

107, 185–196.

- 25 Block MR, Zaccai G, Lauquin GJ & Vignais P V (1982) Small angle neutron scattering of the mitochondrial ADP/ATP carrier protein in detergent. *Biochem. Biophys. Res. Commun.* **109**, 471–477.
- 26 Osborne HB, Sardet C, Michel-Villaz M & Chabre M (1978) Structural study of rhodopsin in detergent micelles by small-angle neutron scattering. *J. Mol. Biol.* **123**, 177–206.
- 27 Nogales A, García C, Pérez J, Callow P, Ezquerra T a & González-Rodríguez J (2010) Three-dimensional model of human platelet integrin  $\alpha$ IIb  $\beta$ 3 in solution obtained by small angle neutron scattering. *J. Biol. Chem.* **285**, 1023–1031.
- 28 Breyton C, Gabel F, Lethier M, Flayhan A, Durand G, Jault J-M, Juillan-Binard C, Imbert L, Moulin M, Ravaud S, Härtlein M & Ebel C (2013) Small angle neutron scattering for the study of solubilised membrane proteins. *Eur. Phys. J. E. Soft Matter* **36**, 71.
- 29 Breyton C, Flayhan A, Gabel F, Lethier M, Durand G, Boulanger P, Chami M & Ebel C (2013) Assessing the conformational changes of pb5, the receptor-binding protein of phage T5, upon binding to its escherichia coli receptor FhuA. *J. Biol. Chem.* **288**, 30763–30772.
- 30 Petoukhov M V., Franke D, Shkumatov A V., Tria G, Kikhney AG, Gajda M, Gorba C, Mertens HDT, Konarev P V. & Svergun DI (2012) New developments in the ATSAS program package for small-angle scattering data analysis. *J. Appl. Crystallogr.* **45**, 342–350.
- 31 Pedersen MC, Arleth L & Mortensen K (2013) WillItFit: A framework for fitting of constrained models to small-angle scattering data. *J. Appl. Crystallogr.* **46**, 1894–1898.
- 32 Curtis JE & Krueger S SASSIE. *NIST*.
- 33 Ilavsky J & Jemian PR (2009) Irena: Tool suite for modeling and analysis of small-angle scattering. *J. Appl. Crystallogr.* **42**, 347–353.
- 34 Schneidman-Duhovny D, Hammel M & Sali A (2010) FoXS: a web server for rapid computation and fitting of SAXS profiles. *Nucleic Acids Res.* **38**, 540–544.
- 35 Darwish TA, Luks E, Moraes G, Yepuri NR, Holden PJ & James M (2013) Synthesis of deuterated [D 32] oleic acid and its phospholipid derivative [D 64] dioleoyl- sn -glycero-3-phosphocholine. *J. Label. Compd. Radiopharm.* **56**, 520–529.
- 36 Koch HJ & Stuart RS (1977) A novel method for specific labelling of carbohydrates with deuterium by catalytic exchange. *Carbohydr. Res.* **59**, C1–C6.
- 37 Hans J. Koch RSS (1978) The synthesis of per-C-deuterated D-glucose. *Carbohydr. Res.* **64**, 127–134.
- 38 Koch H & Stuart R (1978) The catalytic C-deuteration of some carbohydrate derivatives. *Carbohydr. Res.* **67**, 341–348.
- 39 Hansen S (2012) BayesApp : a web site for indirect transformation of small-angle scattering data. *J. Appl. Crystallogr.* **45**, 566–567.
- 40 Malik L, Nygaard J, Hoiberg-Nielsen R, Arleth L, Hoeg-Jensen T & Jensen KJ (2012) Perfluoroalkyl Chains Direct Novel Self-Assembly of Insulin. *Langmuir* **28**, 593–603.
- 41 Pedersen JS (1993) Resolution effects and analysis of small-angle neutron scattering data. *Le J.*

*Phys. IV* **3**, C8-491-C8-498.

- 42 Mylonas E & Svergun DI (2007) Accuracy of molecular mass determination of proteins in solution by small-angle X-ray scattering. *J. Appl. Crystallogr.* **40**, s245–s249.
- 43 Michel H, Oesterhelt D & Henderson R (1980) Orthorhombic two-dimensional crystal form of purple membrane. *Proc. Natl. Acad. Sci. U. S. A.* **77**, 338–42.
- 44 Rasmussen SGF, Choi H-J, Rosenbaum DM, Kobilka TS, Thian FS, Edwards PC, Burghammer M, Ratnala VRP, Sanishvili R, Fischetti RF, Schertler GFX, Weis WI & Kobilka BK (2007) Crystal structure of the human beta2 adrenergic G-protein-coupled receptor. *Nature* **450**, 383–7.
- 45 Schirmer T, Keller TA, Wang YF & Rosenbusch JP (1995) Structural basis for sugar translocation through maltoporin channels at 3.1 Å resolution. *Science* **267**, 512–514.
- 46 Fromme P, Jordan P & Krauß N (2001) Structure of photosystem I. *Biochim. Biophys. Acta - Bioenerg.* **1507**, 5–31.
- 47 Ben-Shem A, Frolov F & Nelson N (2003) Crystal structure of plant photosystem I. *Nature* **426**, 630–5.
- 48 Sobolevsky AI, Rosconi MP & Gouaux E (2009) X-ray structure, symmetry and mechanism of an AMPA-subtype glutamate receptor. *Nature* **462**, 745–756.
- 49 Olesen C, Picard M, Winther A-ML, Gyrop C, Morth JP, Oxvig C, Møller JV & Nissen P (2007) The structural basis of calcium transport by the calcium pump. *Nature* **450**, 1036–42.
- 50 Bublitz M, Musgaard M, Poulsen H, Thøgersen L, Olesen C, Schiøtt B, Morth JP, Møller JV & Nissen P (2013) Ion pathways in the sarcoplasmic reticulum Ca<sup>2+</sup>-ATPase. *J. Biol. Chem.* **288**, 10759–10765.
- 51 Putnam CD, Hammel M, Hura GL & Tainer J a (2007) X-ray solution scattering (SAXS) combined with crystallography and computation: defining accurate macromolecular structures, conformations and assemblies in solution. *Q. Rev. Biophys.* **40**, 191–285.
- 52 Pernot P, Theveneau P, Giraud T, Fernandes RN, Nurizzo D, Spruce D, Surr J, McSweeney S, Round A, Felisaz F, Foedinger L, Gobbo A, Huet J, Villard C & Cipriani F (2010) New beamline dedicated to solution scattering from biological macromolecules at the ESRF. *J. Phys. Conf. Ser.* **247**, 12009.
- 53 Columbus L (2015) Post-expression strategies for structural investigations of membrane proteins. *Curr. Opin. Struct. Biol.* **32**, 131–138.
- 54 Maslennikov I & Choe S (2013) Advances in NMR structures of integral membrane proteins. *Curr. Opin. Struct. Biol.* **23**, 555–562.
- 55 Calcutta A, Jessen CM, Behrens MA, Oliveira CLP, Renart ML, González-Ros JM, Otzen DE, Pedersen JS, Malmendal A & Nielsen NC (2012) Mapping of unfolding states of integral helical membrane proteins by GPS-NMR and scattering techniques: TFE-induced unfolding of KcsA in DDM surfactant. *Biochim. Biophys. Acta* **1818**, 2290–301.
- 56 Døvling Kaspersen J, Moestrup Jessen C, Stougaard Vad B, Skipper Sørensen E, Kleiner Andersen K, Glasius M, Pinto Oliveira CL, Otzen DE & Pedersen JS (2014) Low-Resolution Structures of OmpA-DDM Protein-Detergent Complexes. *ChemBioChem* **15**, 2113–2124.
- 57 Berthaud A, Manzi J, Pérez J & Mangenot S (2012) Modeling detergent organization around

aquaporin-0 using small-angle X-ray scattering. *J. Am. Chem. Soc.* **134**, 10080–8.

- 58 Bu Z & Engelman DM (1999) A method for determining transmembrane helix association and orientation in detergent micelles using small angle x-ray scattering. *Biophys. J.* **77**, 1064–1073.
- 59 Skar-Gislinge N, Simonsen JB, Mortensen K, Feidenhans'l R, Sligar SG, Lindberg Møller B, Bjørnholm T & Arleth L (2010) Elliptical structure of phospholipid bilayer nanodiscs encapsulated by scaffold proteins: casting the roles of the lipids and the protein. *J. Am. Chem. Soc.* **132**, 13713–22.
- 60 Jordan A, Jacques M, Merrick C, Devos J, Forsyth VT, Porcar L & Martel A (2016) SEC-SANS: size exclusion chromatography combined in situ with small-angle neutron scattering. *J. Appl. Crystallogr.* **49**, 2015–2020.
- 61 Glasoe PK & Long FA (1960) Use of glass electrodes to measure acidities in deuterium oxide. *J. Phys. Chem.* **64**, 188–190.
- 62 Armarego WLF & Perrin DD *Purification of Laboratory Chemicals*, Fourth Ed. Elsevier.
- 63 Gilbert EP, Schulz JC & Noakes TJ (2006) "Quokka"-the small-angle neutron scattering instrument at OPAL. *Phys. B Condens. Matter* **385–386**, 1180–1182.
- 64 Franke D & Svergun DI (2009) DAMMIF, a program for rapid ab-initio shape determination in small-angle scattering. *J. Appl. Crystallogr.* **42**, 342–346.
- 65 Adams PD, Afonine P V., Bunkóczi G, Chen VB, Davis IW, Echols N, Headd JJ, Hung LW, Kapral GJ, Grosse-Kunstleve RW, McCoy AJ, Moriarty NW, Oeffner R, Read RJ, Richardson DC, Richardson JS, Terwilliger TC & Zwart PH (2010) PHENIX: A comprehensive Python-based system for macromolecular structure solution. *Acta Crystallogr. Sect. D Biol. Crystallogr.* **66**, 213–221.
- 66 Lomize MA, Lomize AL, Pogozheva ID & Mosberg HI (2006) OPM: Orientations of proteins in membranes database. *Bioinformatics* **22**, 623–625.

	OG		DDM	
	head group	tail group	head group	tail group
Chemical composition of the detergent component	$C_2H_{11}O_6$	$C_8H_{17}$	$C_{12}H_{21}O_{11}$	$C_{12}H_{25}$
Exchangeable hydrogens	4	0	7	0
Theoretical level of deuteration needed for match-out at 100% D <sub>2</sub> O	$C_6D_{7.6}H_{3.4}O_6$	$C_8D_{15.9}H_{1.1}$	$C_{12}D_{15.2}H_{5.8}O_{11}$	$C_{12}D_{22.4}H_{2.6}$
Experimentally obtained level of deuteration in 100% D <sub>2</sub> O	$C_6D_{7.64}H_{3.36}O_6$	$C_8D_{15.98}H_{1.12}$	$C_{12}D_{14.98}H_{6.02}O_{11}$	$C_{12}D_{22.25}H_{2.75}$

Table 1: Deuteration levels needed and obtained for *n*-octyl β-D-glucopyranoside (OG) and *n*-dodecyl-β-D-maltopyranoside (DDM).

	$R_g$ exp. [Å]	$R_g$ calc. [Å]	$D_{max}$ exp. [Å]	$D_{max}$ calc. [Å]	$MW$ exp. [kDa]	$MW$ calc. [kDa]
bR	$21.6 \pm 0.04$	17.4	$60.2 \pm 0.9$	53	44.6	27
LamB	$57.9 \pm 0.2$	33.4	$201 \pm 1$	87	210	47
PSI	$55.2 \pm 0.2$	51.3	$199 \pm 5$	159	473	650
GluA2	$60.0 \pm 0.4$	56.2	$166 \pm 1$	173	278	385
SERCA E1 + E2	$56.4 \pm 0.1$	38.4	$204.5 \pm 0.6$	123	460	110

**Table 2: Structural parameters deduced from the experimental data and the calculated theoretical values from the fitted models as obtained through Indirect Fourier Transform.  $R_g$ : Radius of gyration.  $D_{max}$ : Maximum distance present in the scattering particle. MW: Molecular weight. Experimental values obtained from SANS data, theoretical values calculated from the available crystal structures.**

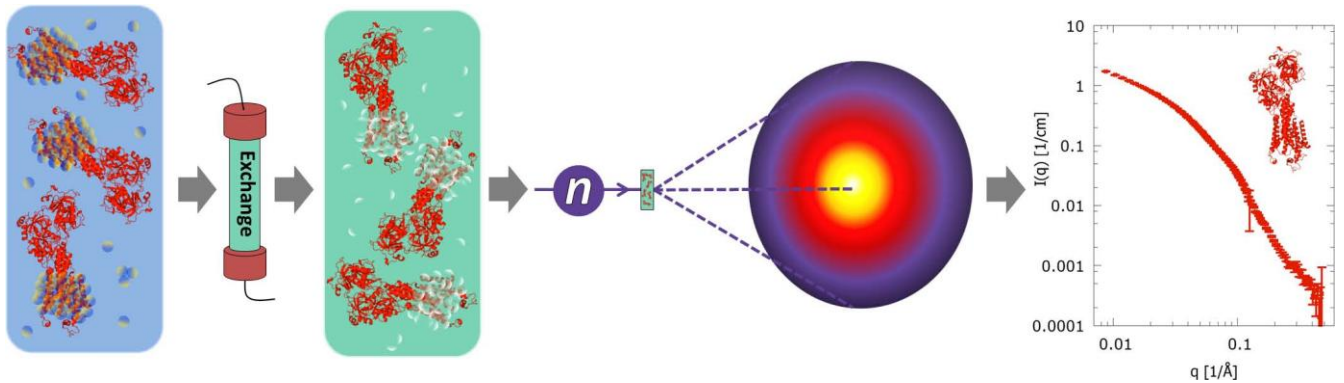


**Figure 1: Process outline of the experiment. Initially, the membrane protein is in  $H_2O$  based buffer and hydrogenated detergents. This sample is then applied to a size exclusion column equilibrated in  $D_2O$  based buffer and the match-out deuterated detergents, allowing the hydrogenated buffer and detergent to be exchanged to their deuterated counterparts. The obtained sample is used directly for SANS measurements to obtain a single contrast dataset yielding only the scattering from the membrane protein. Data from the experiment can then be analyzed by generally available software developed for determining the low resolution structure of proteins in solution.**

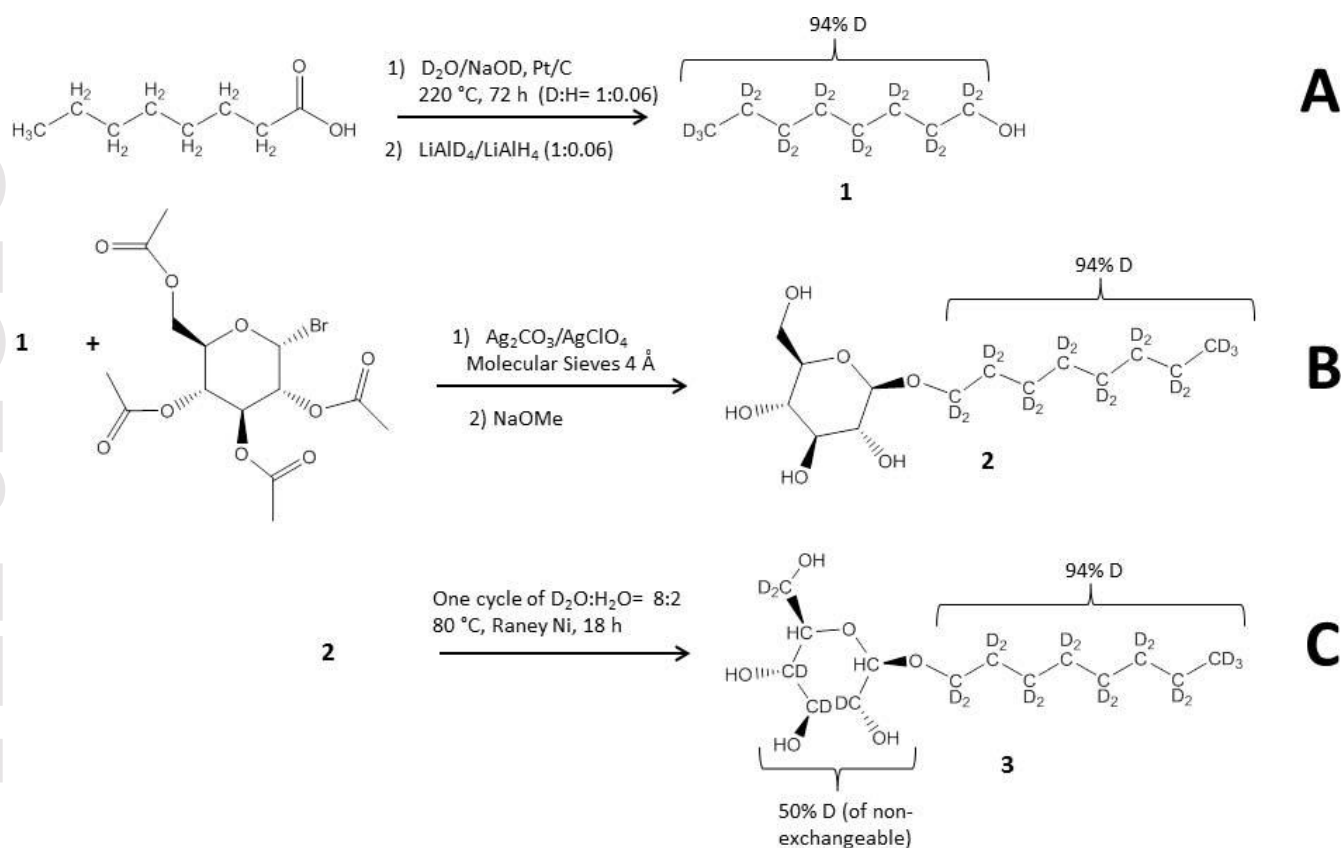


**Figure 2.** Reaction scheme for the synthesis of specifically deuterated levels of OG (the corresponding scheme for DDM can be found in Figure S1). Step A) The fatty acid is deuterated by Pt/C catalyzed H/D exchange reactions at  $220^\circ\text{C}$  to produce the correctly deuterated version and then it is reduced to the corresponding alcohol (**1**) using the specified D:H ratio. Step B) The deuterated alcohol (**1**) is coupled to the acetylated bromo-sugar head-group, producing the tail deuterated version of the detergent, which is then deacetylated to produce (**2**). Step C) The sugar head group is deuterated via Raney Nickel catalysis to produce the final partially deuterated detergent (**3**) with different levels of deuteration in the head and the tail groups.

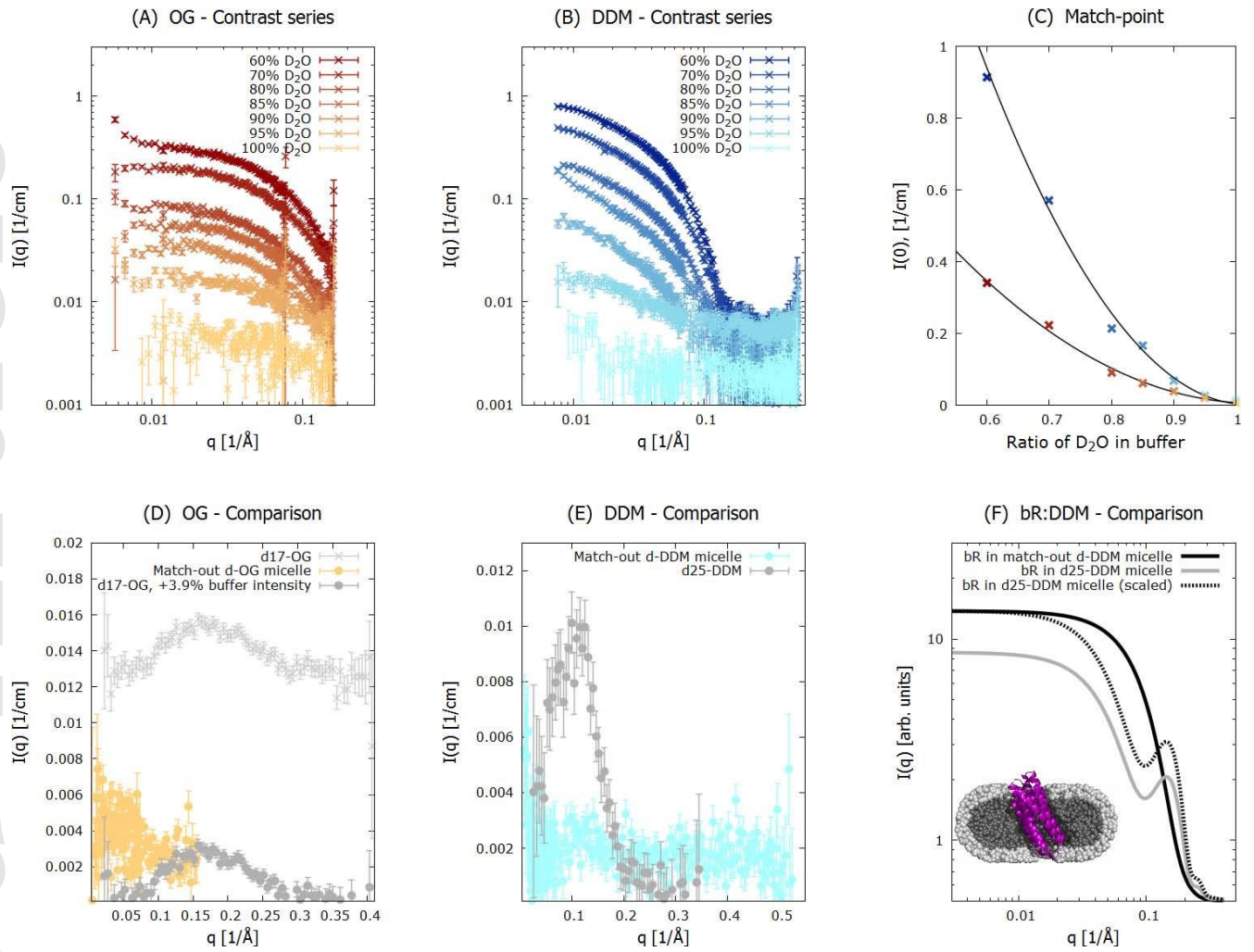


**Figure 3:** (A) Background subtracted SANS data from match-out deuterated OG in increasing percentage of D<sub>2</sub>O in the buffer. (B) SANS data from match-out deuterated DDM in increasing percentage of D<sub>2</sub>O in the buffer. (C) Experimental  $I(0)$  values plotted (points) and the corresponding quadratic power law fits (lines). (D) Comparison of  $I(q)$  from match-out d-OG (yellow) and d17-OG (light and dark grey), both measured at their match-point. Light-grey curve plots d17-OG with the usual background subtraction. In the dark grey curve the d17-OG background has been empirically increased by a factor of 1.039. (E) Comparison of match-out d-DDM (turquoise) and d25-DDM (grey) measured at its match-point. Data from d17-OG and d25-DDM are reproduced from [28]. (A)-(E) Errorbars are the standard deviation (SD), obtained from counting statistics and standard error propagation. (F) Simulation of a Bacteriorhodopsin monomer measured by SANS in respectively match-out d-DDM (black) and in d25-DDM (grey and dashed) micelles.

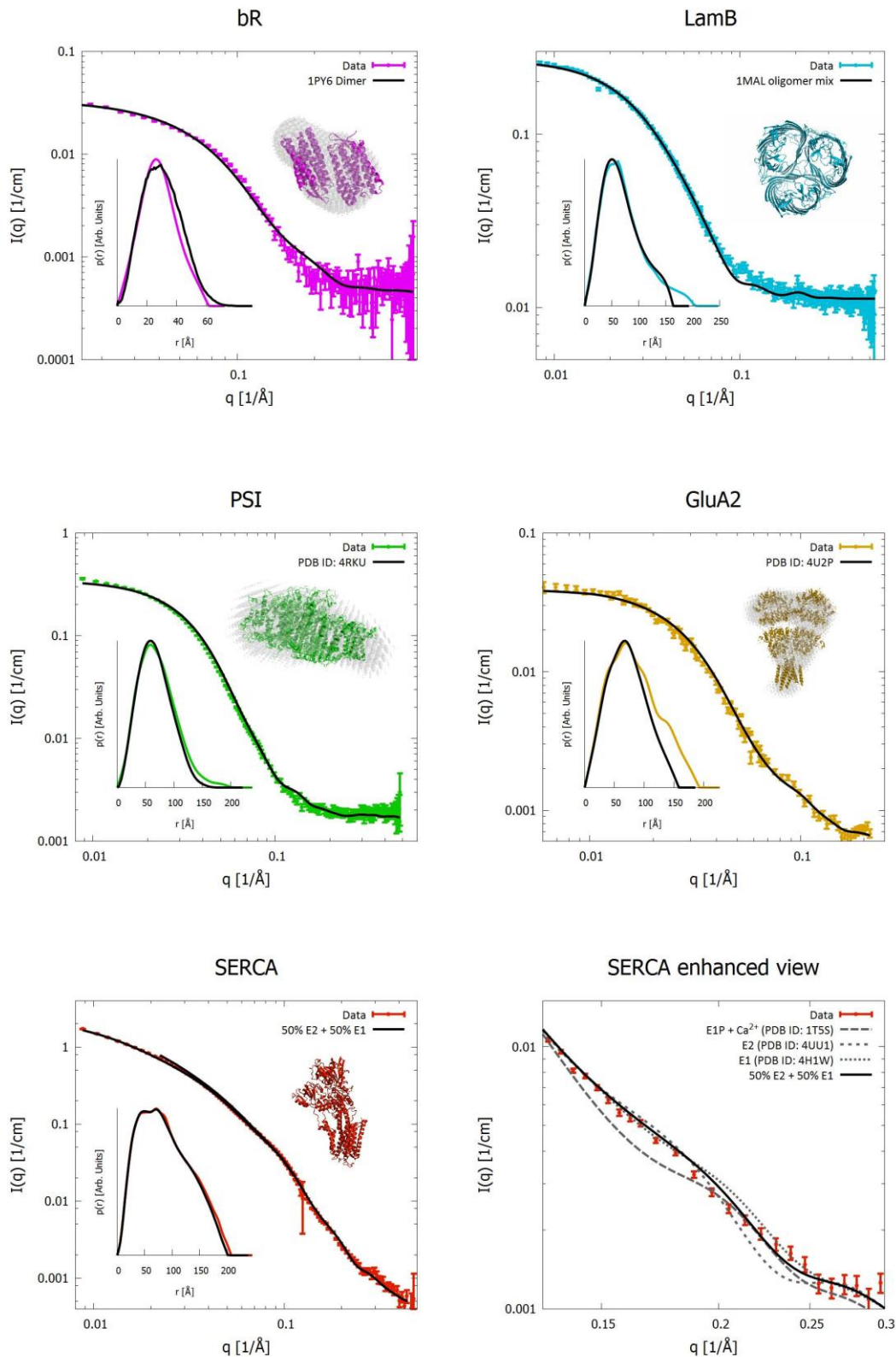


**Figure 4: Experimental SANS data (colored points) and the resulting model fits (black full and dashed lines) for the five investigated membrane proteins. Errorbars are the standard deviation (SD), obtained from counting statistics and standard error propagation. Note that instrumental resolution effects are included in the models, which then exhibit small discontinuities at medium  $q$ -values. Inserts: The corresponding pair-distance distribution functions as determined by Indirect Fourier transform[39] with identical color scheme. Figures are the known structures from crystallography together with the *ab initio* bead models where appropriate. Note that SERCA (data, model and  $p(r)$ ) contain a fraction of aggregated protein.**